PHOENIX-XNS – A MINIATURE REAL-TIME NAVIGATION SYSTEM FOR LEO SATELLITES

Oliver Montenbruck, Eberhard Gill, Markus Markgraf

Deutsches Zentrum für Luft- und Raumfahrt (DLR), German Space Operations Center(GSOC)
D-82234 Wessling, Germany
Email: oliver.montenbruck@dlr.de

ABSTRACT

The paper describes the development of a miniature GPS receiver with integrated real-time navigation system for orbit determination of satellites in low Earth orbit (LEO). The Phoenix-XNS receiver is based on a commercial-off-the-shelf (COTS) single-frequency GPS receiver board that has been qualified for use in a moderate space environment. Its firmware is specifically designed for space applications and accounts for the high signal dynamics in the acquisition and tracking process. The supplementary eXtended Navigation System (XNS) employs an elaborate force model and a 24-state Kalman filter to provide a smooth and continuous reduced-dynamics navigation solution even in case of restricted GPS availability. Through the use of the GRAPHIC code-carrier combination, ionospheric path delays can be fully eliminated in the filter, which overcomes the main limitation of conventional single-frequency receivers. Tests conducted in a signal simulator test bed have demonstrated a filtered navigation solution accuracy of better than 1 m (3D rms).

INTRODUCTION

The Phoenix GPS receiver (Fig. 1) is a miniature Global Positioning System receiver specifically designed for high dynamics applications such as sounding rockets and satellites in low Earth orbit [1]. The receiver is based on SigTech's commercial-off-the-shelf MG5001 receiver board and has been qualified for space use in a series of thermal-vacuum, vibration and total ionization dose tests. It employs a GP4020 baseband processor which combines a 12 channel GP2021 correlator and an ARM7TDMI microprocessor kernel. At a power consumption of less than one Watt and a board size of 50 x 70 mm the receiver is among the smallest of its kind and particularly well suited for satellites with limited onboard resources. The Phoenix receiver is extensively used in European sounding rocket missions and has been selected for the Proba-2, X-Sat, ARGO, and Flying Laptop micro-satellites as well as the PRISMA formation flying mission.

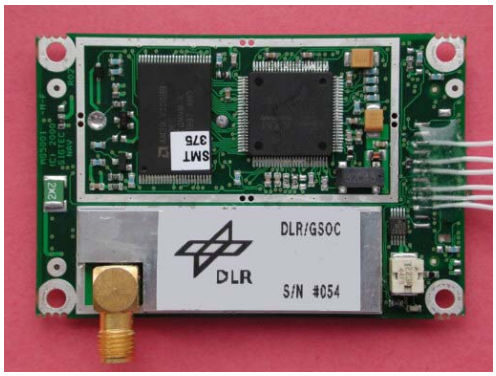

Fig. 1 Phoenix GPS receiver board

The Phoenix-XNS receiver provides a 512 kByte flash EPROM for the receiver software, which enables in-flight updates of the firmware via the onboard data handling system. Compared to a standard MG5001 board, RAM memory for run-time code and data has been doubled (512 kB) for operation of the XNS software. Supplementary to the external memory modules, the GP4020 chip provides a fast internal RAM of 32 kByte size. It can be maintained by a backup battery or keep-alive line and serves as non-volatile memory for critical receiver parameters such as almanac, broadcast ephemerides and orbit elements of the user spacecraft. Likewise a 32.768 kHz clock crystal and a real-time clock (RTC) inside the GP4020 can be used to maintain the current time during deactivation of the main power supply.

As mentioned before, the receiver is specifically designed to work under specific signal conditions of LEO satellite applications. Besides an internal orbit propagator for initial acquisition aiding, the receiver offers a wide-band 3rd order phase-locked loop with frequency-locked loop assist for carrier tracking and a narrow-band carrier aided delay-lock loop for code tracking. This ensures robust tracking and avoids systematic steady state errors even under high signal dynamics. All measurements are synchronized to integer GPS seconds with a representative accuracy of 0.2μs and a

one-pulse-per-second hardware signal is generated at the same instant. The tracking loop design enables code and carrier measurements with a noise level of 0.4 m (pseudorange) and 0.5 mm (carrier phase) at a representative carrier-to-noise-density ratio of 45 dBHz. Carrier phase measurements are, furthermore, ensured to exhibit integer double-difference ambiguities. This allows use of the Phoenix receiver for carrier phase differential GPS applications such as formation flying and attitude determination.

Despite a high raw data quality, the achievable single-point navigation accuracy is, however, limited to typically 10m (3D rms) due to broadcast ephemeris errors and unaccounted ionospheric path delays. To cope with these limitations, the eXtended Navigation System (XNS) for the Phoenix receiver has been developed. The navigation system makes use of an extended Kalman filter which provides a dynamical smoothing of the raw GPS measurements. Benefits of the dynamical filtering include a substantial noise reduction and the capability to bridge periods of poor GPS visibility or outages through numerical propagation of the orbit. Furthermore, the filter supports the elimination of ionospheric path delays. The XNS functionality is embedded into the standard firmware and can be executed on Phoenix receiver boards with increased (512kB) RAM memory.

XNS NAVIGATION SOFTWARE

Software Architecture

The XNS consitutes an enhancement and extension of the basic Phoenix GPS receiver firmware. To keep a clear separation between the core receiver software and the navigation software, the latter is treated as an additional task running on the processor with a minimum of interfaces between the two parts (Fig. 2). Besides XNS-specific commands and messages, the core receiver software does not depend on any function or result related to the real-time navigation software. The navigation software, on the other hand, benefits from an easy access to GPS raw data and auxiliary information through a data pool provided by the core receiver software.

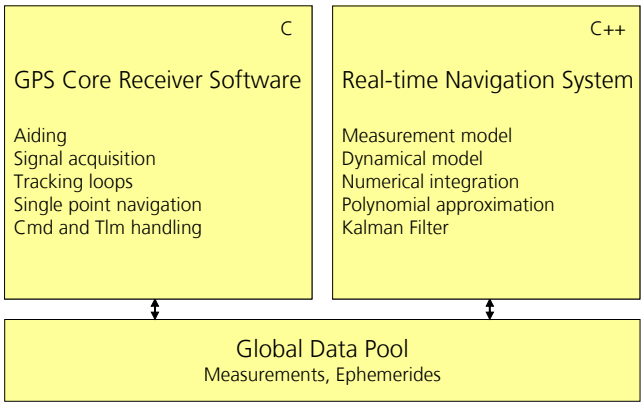

Fig. 2 XNS basic software architecture

A language mixing has been adopted with the core receiver software implemented in ANSI C and the navigation software based on C++. Key parts of the navigation software comprise the GPS measurement model, the dynamic model of the spacecraft motion, the numerical integration and polynomial approximation of the trajectory, as well as the measurement filtering. Whereas the core receiver software employs static variables exclusively, the real-time navigation software is allowed to make use of dynamical memory. Long-term tests (24h) conducted in a signal simulator test bed indicate a proper garbage collection and flawless execution of the receiver software.

Filter Design

The XNS comprises an extended Kalman filter, which performs a dynamical smoothing of raw GPS measurements. Other than common navigation systems for single-frequency receivers, the XNS does not process pseudorange measurements directly. Instead, it employs a linear combination of GPS L1 C/A code and carrier phase, which is known as GRAPHIC (Group and Phase Ionospheric Correction) measurement [2]. This combination is based on the consideration that carrier phases exhibit a phase change in dispersive media that is equal in size to the code delay I, but opposite in sign. Denoting the range between the GPS satellite and the receiver by ρ, the GPS and receiver clock offsets by cdt_{GPS} and cdt, and the carrier phase bias by $n\lambda$, the code and carrier measurements can be expressed as

$$\begin{aligned} \rho^{\mathrm{C/A}} &= \rho + c(\delta t - \delta t_{\mathrm{GPS}}) + I \\ \rho^{\mathrm{L1}} = \lambda\varphi &= \rho + c(\delta t - \delta t_{\mathrm{GPS}}) - I + n\lambda \ . \end{aligned} \tag{1}$$

The ionospheric range delay can thus be fully eliminated by forming the arithmetic mean

$$\rho^* = (\rho^{C/A} + \rho^{L1})/2 = \rho + c(\delta t - \delta t_{GPS}) + B \quad (2)$$

with $B=n/2$. This approach, removes the dominant systematic error source for single-frequency GPS measurements and is vital for achieving accurate navigation results. Use of GRAPHIC data is also beneficial in terms of the measurement noise, which is 50% smaller than the pseudorange noise (i.e. about 0.2-0.3 m for the Phoenix receiver). On the other hand, the carrier phase ambiguity results in an unknown bias of the GRAPHIC measurements for each tracking channel. These biases have to be estimated along with the other state and model parameters and result in a corresponding increase of the filter dimension. Even though the benefits of GRAPHIC observables have been emphasized by various authors [3,4], the technology has hardly found its way into practical real-time navigation systems so far.

The dynamical trajectory model adopted in the XNS accounts for the aspheric gravitational potential of the Earth, luni-solar gravitational perturbations, solar radiation pressure and atmospheric drag using a Harris-Priester model [5]. For use at low altitudes, a GGM01S gravity field model up to degree and order 50 is employed [6] and solid Earth tides can be incorporated as needed. To minimize the impact of reference system transformation uncertainties, the equation of motion is consistently formulated in a co-moving Earth-fixed coordinate system with proper account of centrifugal and Coriolis accelerations. Even though UT1 and polar motion data can be provided via the XNS command interface if deemed necessary, the filtered state in the Earth-fixed system is essentially insensitive to errors in these parameters.

Remaining imperfections of the dynamical model (caused mainly by a simplified treatment of spacecraft surface forces) are compensated by empirical accelerations in radial, tangential and normal direction. These accelerations are treated as exponentially correlated random variables in the extended Kalman filter. In total, the filter state comprises

- 6 position-velocity components,
- 1 radiation pressure coefficient
- 1 drag coefficient,
- 3 empirical accelerations,
- 1 clock offset and
- 12 GRAPHIC biases

that are simultaneously adjusted from the GPS measurements. Within the time update step, the clock offset is treated as a white noise process, while the empirical accelerations are treated as exponentially correlated random variables [7,8].

For the numerical integration of the equation of motion the XNS employs an advanced numerical integration scheme (RK4R), which extends the common Runge-Kutta 4th order algorithm (RK4) by a Richardson extrapolation and a Hermite interpolation [9]. The algorithm comprises two elementary RK4 step sizes of length h and can be shown to be effectively of 5th order with six function calls per h. The Hermite interpolation of the spacecraft position allows for an efficient provision of dense position-velocity output which is commonly required by spacecraft attitude control systems.

The state transition matrix between filter updates and the sensitivity matrix are likewise obtained from a numerical integration, albeit with a simplified force model that accounts only for the dominant Earth oblateness perturbations.

Real-Time Tasking Concept

Compared to single point navigation solutions, which are performed once per second in the Phoenix receiver, the computation of a filtered navigation solution is much more demanding in terms of computational resources. Even though a spare computing time of about 50% is available during normal Phoenix operations, the remaining processor capacity is insufficient to perform the XNS trajectory prediction and filter update at each second.

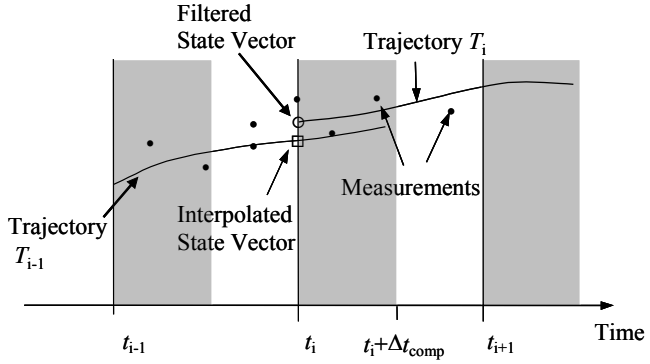

Fig. 3 XNS processing timeline (from [10])

To cope with this situation a tailored real-time operations concept for onboard navigation systems has earlier been developed in the context of the BIRD mission [10]. The navigation software is actually operated as a slow background task with an activation interval of typically 30s. This interval reflects a natural step size for the numerical integration of the trajectory and provides a proper trade-off between accuracy, computational effort and response time of the filter. As illustrated in Fig. 3, the filter is invoked at discrete intervals (t_i) where the state vector is obtained from an interpolation of the previous cycle. Following the measurement update, an improved (filtered) state vector at t_i is available. This state is then integrated to t_i+h which is beyond the time t_{i+1} of the next processing step. The total processing time Δt_{comp} of the XNS task is indicated by the shaded areas in Fig. 3. It may vary between 20% and 70% of a task cycle period, depending on the complexity of the employed force model.

As part of the numerical integration process, a continuous polynomial representation of the trajectory between t_i and t_{i+1}+h is made available by the RK4R integrator, which serves as starting point for the next Kalman update and orbit prediction step. At an integration step size of h=65s the trajectory polynomial covers at least two task intervals, which ensures availability of a filtered navigation solution irrespective of the actual computational load. The trajectory polynomials furthermore allow the computation of (interpolated/predicted) state vectors that are fully synchronized with the update rate and the epochs of the kinematic navigation solution.

The above scheme implies that only one set of GPS raw measurements is processed per cycle. For convenience, the task start time and the corresponding GPS measurement epoch are synchronized to integer half-minutes of GPS time and a measurement coinciding with this epoch is generally used for the state update. For initialization of the filter, the latest kinematic navigation solution of the Phoenix receiver is employed as a priori information. It has a representative accuracy of 10 m and 0.1 m/s, respectively, and is used initially to predict the trajectory of the user spacecraft over a time interval of 65s. Raw GPS measurement can then be processed at the next activation of the XNS task.

XNS OPERATIONS

Start-Up and Initialization

After booting the Phoenix receiver, the navigation task remains in a stalled mode. While activated at regular 30s intervals, the task performs no computational actions and control is immediately passed backed to the next higher-priority task. To “wake-up” the XNS task, an explicit initialization has to be performed. For most applications, an auto-initialization is adequate, which means that the initial spacecraft state is taken from the latest available single-point navigation solution. An auto-initialization is requested by issuing a parameter-less initialization command and takes effect upon the next activation of the XNS task. If the receiver has not yet achieved a valid navigation fix, the auto-initialization is deferred and tried again at each subsequent task activation.

As an alternative, an epoch and ECEF state vector may be passed to the receiver as part of the initialization command, in which case the trajectory is initialized with the specified position and velocity information. The user input must be properly synchronized with the receiver time at command execution and initialization commands are rejected if a specified epoch differs by more than 60s from the current time.

Filtered Navigation Solution

For operational onboard use, the XNS software offers a filtered navigation solution message, which matches the structure and format of the kinematic single-point navigation solution of the standard Phoenix receiver. The filtered navigation solution is based on an interpolation of the predicted trajectory after the latest measurement update. It can thus be output at a user selectable data rate (up to 1 Hz) irrespective of the actual update cycle of the Kalman filter.

Filter Tuning

The XNS navigation filter involves a large number of tunable parameters describing the statistical properties of measurements, a priori information, and process noise. A mission specific default parameter set is encoded in the software and made available at boot time. The current settings are summarized in a dedicated output message and can, at any time, be queried with the XNPAR command. The XNPAR command also allows the change of individual parameters at run time. Updates take effect during the command processing and may thus affect an ongoing filter or measurements step. It is therefore preferable to update filter parameters only when the XNS task is stalled. The XNPAR command can also be used to provide UT1 time and polar motion information to the XNS and to select the degree and order of the employed gravity field model.

VALIDATION AND TESTING

The Phoenix receiver has undergone extensive testing in a signal simulator test bed to assess the performance of the signal tracking software and the navigation filter. A Spirent STR4500 12-channels, L1-C/A-code signal generator was employed along with pre-computed test scenarios generated on an STR7790 simulator. The adopted scenario reflects a Sun-synchronous spacecraft at 400 km altitude and has earlier been defined in the context of the Aeolus mission [11]. The start epoch is chosen as 1 Oct. 2008, 0:00 GPS Time, and coincides with the descending node crossing.

The orbit is propagated by the simulator using a JGM-3 40 x 40 Earth gravity model as well as drag perturbations. Supplementary to the orbital parameters, the ballistic properties of the satellite were defined by assumed values of A=8 m^2, m=1300 kg, C_D=2.3. The generated trajectory is available as output of the signal simulator and provides the primary reference for the Phoenix GPS receiver analysis. Trajectory models used inside the signal simulator are intentionally different from the XNS models described above to enable an unbiased and realistic assessment of the Kalman filter performance

Broadcast ephemeris errors were simulated by offsets of the simulated GPS satellite positions from the values described by the broadcast ephemerides. In accord with the present performance the GPS control segment [12,13], the offsets have been chosen such as to give an average User Equivalent Range Error (UERE) of 1.5m.

Ionospheric path delays were modelled through a constant vertical path delay of 1.64m (corresponding to a Vertical Total Electron Content of 10 TECU) and a Lear mapping function [14]. The simplified ionosphere model is certainly not representative for true satellite missions, but fully adequate to demonstrate the benefit of GRAPHIC measurement for the elimination of ionospheric path delays.

Table 1 XNS filter parameters for Aeolus test scenario

Parameter	Value	Description
n_{grav}	40	Degree and order of gravity field model
σ_{obs}	0.25 m	Standard deviation of GRAPHIC measurements
$\sigma_{apr}(\mathbf{r})$	100 m	Standard deviation of a priori position
$\sigma_{apr}(\mathbf{v})$	0.1m	Standard deviation of a priori velocity
$\sigma_{apr}(C_R)$	0.1	Standard deviation of a priori radiation pressure coefficient
$\sigma_{apr}(C_D)$	0.1	Standard deviation of a priori drag coefficient
$\sigma_{apr}(a_R, a_T, a_N)$	(100,200,200) nm/s^2	Standard deviation of a priori empirical acceleration in RTN direction
$\sigma_{apr}(cdt)$	100 m	Standard deviation of a priori clock offset
$\sigma_{apr}(B)$	2.0 m	Standard deviation of a priori ambiguity
τ_a	600 s	Autocorrelation time of empirical accelerations
$\sigma(a_R, a_T, a_N)$	(10,100,100) nm/s^2	Steady state standard deviation of empirical acceleration in RTN direction
τ_{cdt}	60 s	Reference time interval for clock offset process noise
σ_{cdt}	5 m	Standard deviation of clock offset process noise within reference time interval

Settings of the XNS configurable parameters as used in the Aeolus test case are collated in Table 1. While the degree and order of the XNS gravity field model matches that of the simulator, the model coefficients (GGM01 versus JGM3) are sufficiently different to provide a realistic test case. The GRAPHIC data weight of 25 cm reflects the average pseudorange noise under the given signal strength. Loose a priori constraints for the initial position and velocity have been chosen which well exceed the error of the kinematic navigation solution of the Phoenix receiver. Process noise values for the empirical accelerations are based on expected modeling differences between the simulator and the XNS software. The small process noise value for the clock offset reflects the fact that the Phoenix measurements are referred to a modeled receiver clock which is steered to GPS time based on the kinematic navigation solution.

The error of the filtered navigation solution for the Aeolus simulation is shown in Figs. 4 and 5 for the radial, tangential and normal direction. Following an initial acquisition phase of about 30 min, the filter achieves a steady state performance of about 0.7 m and 1 mm/s 3D rms. The initial position error reflects the error of the kinematic position navigation solution that was used as a priori value for the filter initialization. As a result of the ionospheric path delays the kinematic solution exhibits a mean error of about 6 m in the radial direction (cf. Table 3).

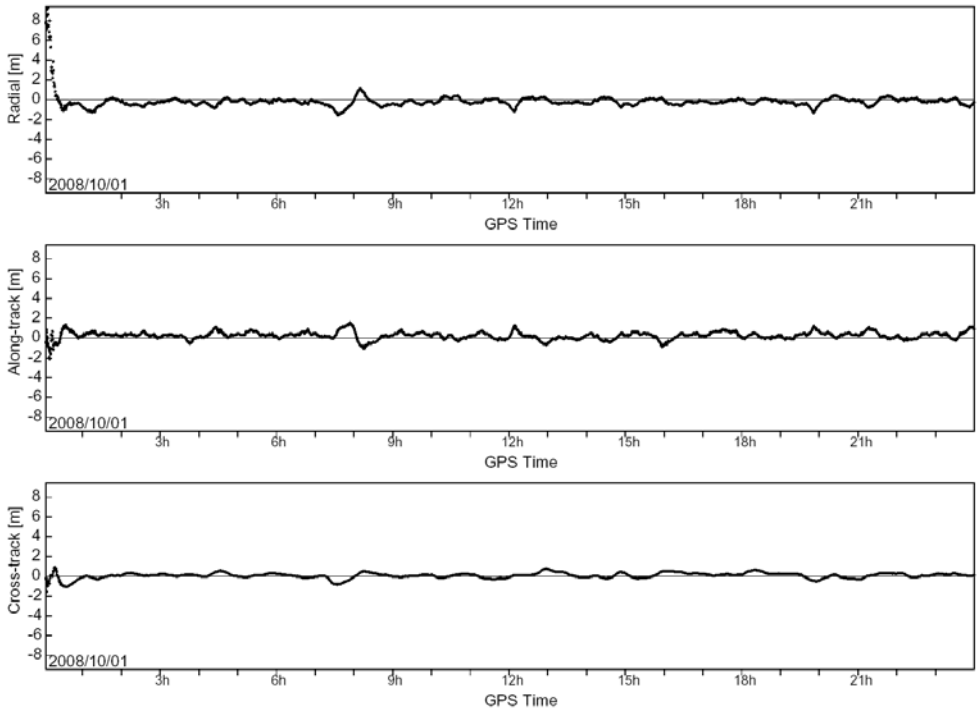

Fig. 4 Error of the filtered Phoenix XNS position solution in radial, tangential (along-track) and normal (Cross-track) direction

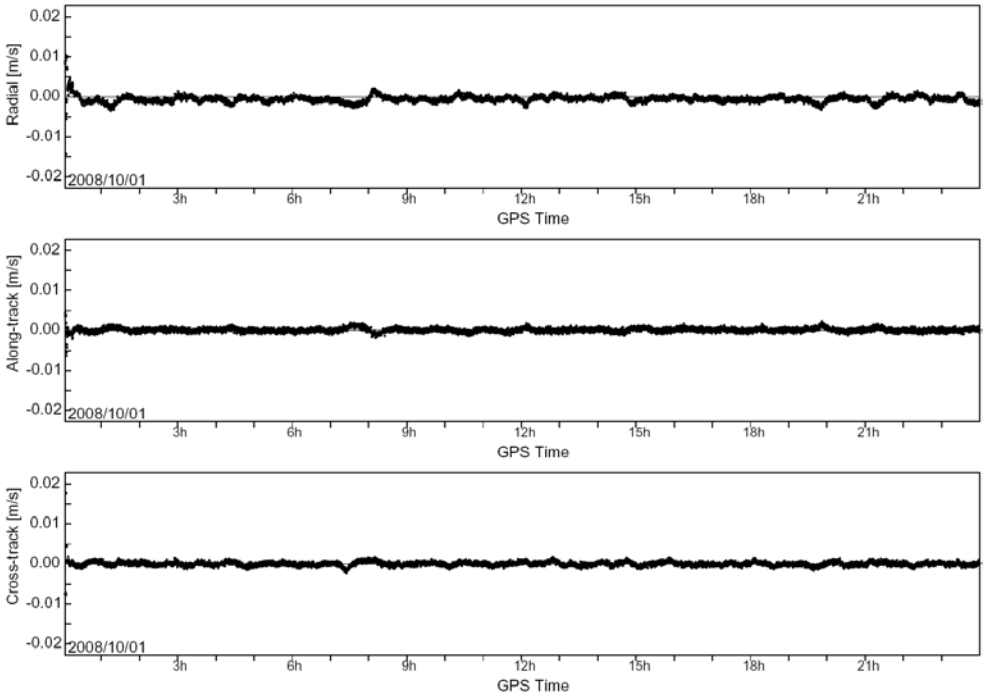

Fig. 5 Error of the filtered Phoenix XNS velocity solution in radial, tangential (along-track) and normal (Cross-track) direction

Table 3 Comparison of the kinematic and dynamically filtered navigation solution accuracy for a one day arc of the Aeolus simulation. Data from the first 30 mins have been ignored to mask the initial acquisition phase of the filter.

Solution	**Radial [m]**	**Along-track [m]**	**Cross-track [m]**	**Position (3D rms)**
kinematic	+6.02 ± 3.79	-1.84 ± 1.51	+0.06 ± 1.35	7.62 m
dynamic	-0.22 ± 0.34	+0.27 ± 0.36	+0.08 ± 0.27	0.67 m
Solution	**Radial [m/s]**	**Along-track [m/s]**	**Cross-track [m/s]**	**Velocity (3D rms)**
kinematic	+0.005 ± 0.040	-0.015 ± 0.019	+0.000 ± 0.015	0.049 m/s
dynamic	-0.001 ± 0.001	+0.000 ± 0.000	+0.000 ± 0.001	0.001 m/s

Compared to the kinematic position (Fig. 6) the filtered position solution is smooth and continuous. The absence of a systematic radial bias underlines the proper elimination of ionospheric path delays through the use of GRAPHIC observables. At the same time the filtered velocity solution provides a noise level of typically 1 mm/s which constitutes a one-to two orders of magnitude improvement over the kinematic solution and enables accurate orbit predictions over extended time intervals.

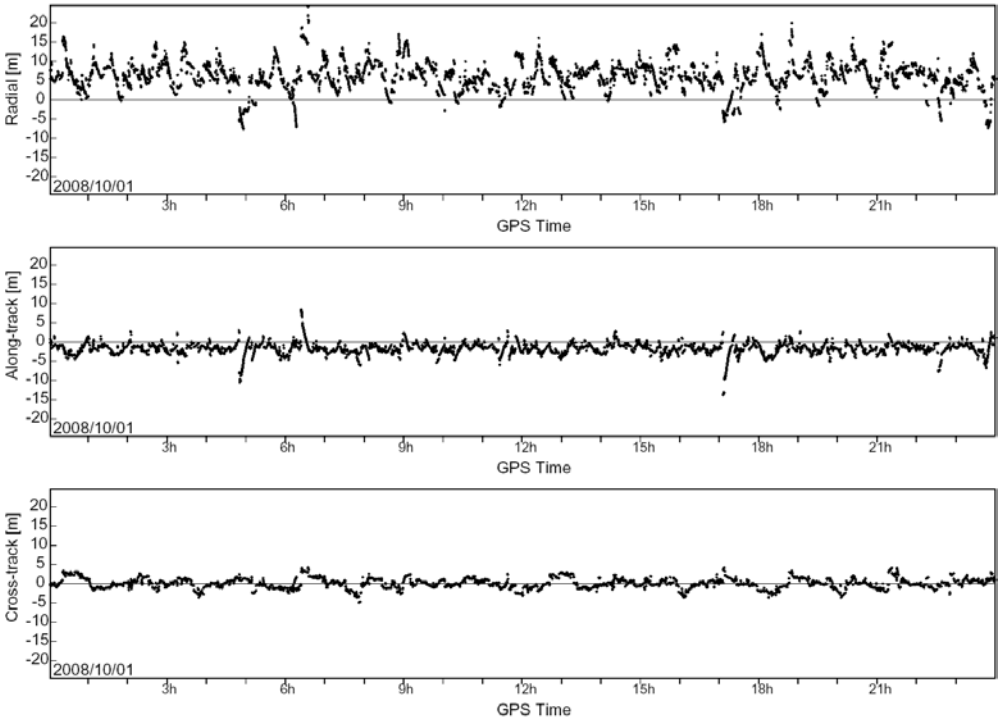

Fig. 6 Error of the unfiltered, kinematic position solution of the Phoenix receiver in the Aelous scenario.

For further reference, the empirical accelerations estimated by the filter are shown in Fig. 7. The along-track and cross-track accelerations exhibit an rms amplitude of 22 nm/s^2 and 44 nm/s^2, respectively, which basically reflects the difference between the dynamical models of the simulator truth and the XNS navigation filter. The radial component, in contrast is effectively constrained to near zero by the adopted priori variance and process noise. Due to a dynamical coupling with the along-component it cannot well be estimated in practice and any radial accelerations are effectively absorbed in the estimated along-track values.

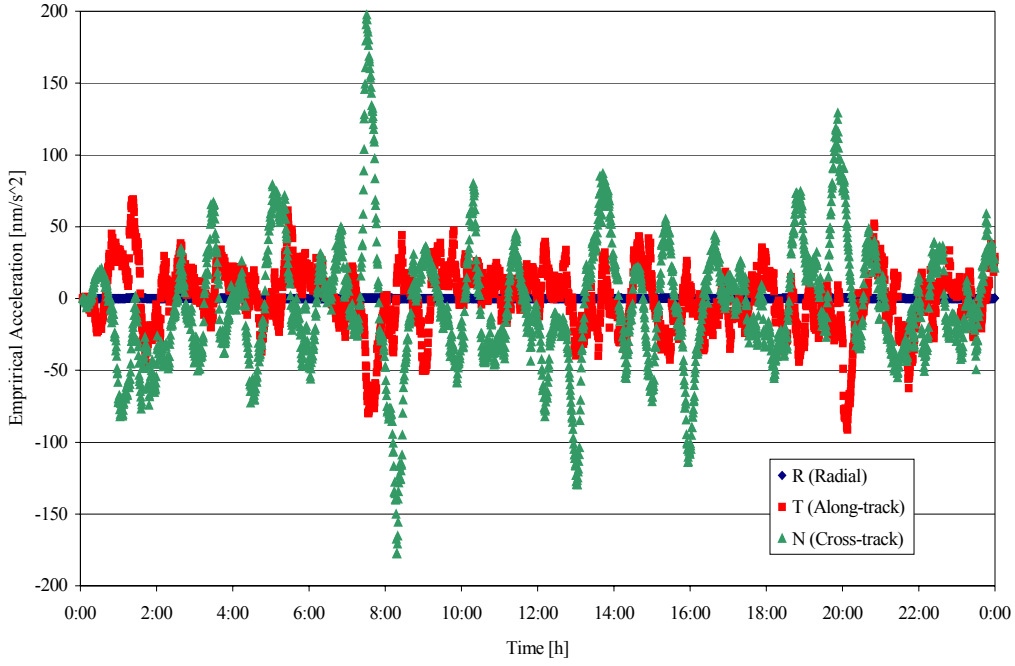

SUMMARY AND OUTLOOK

The standard signal processing and tracking software of the Phoenix GPS receiver has been supplemented by a dynamical filter for real-time orbit determination. Despite the use of single-frequency measurements, ionospheric path delays can be rigorously eliminated through the use of the ionosphere-free code-carrier combination (GRAPHIC). While the need to adjust a separate GRAPHIC bias for each tracking channel increases the filter complexity and results in a 24-dimensional filter state, the system has so far demonstrated a stable and robust performance. Signal simulator tests for a polar LEO orbit at 400km altitude have demonstrated a proper performance of the eXtended Navigation System for the Phoenix GPS receiver. Position errors of 0.5-1m (3D rms) have been obtained after filter convergence in the presence of broadcast ephemeris errors with a user equivalent range error of 1.5m and a thin layer ionosphere with a VTEC of 10 TECU.

The Phoenix XNS software will first be flown onboard the Proba-2 satellite, which is due for launch in mid 2007 [15]. In accord with the primary payload requirements, one axis of the spacecraft will always be pointed towards the Sun. By stepwise rotation about the Sun axis, it will, however, be assured that the star trackers and GPS antenna will always have a proper sky visibility. While less favorable than a strictly zenith pointing antenna, a minimum of four GPS satellites can be tracked at any instance in this configuration. Due to a wide elevation range (-20° to +90°) of the observed satellites, ionospheric path delays will be more pronounced than usually encountered in the same orbit. This will provide a good basis for demonstrating the benefits of GRAPHIC measurements and the capability of a low budget receiver to achieve accurate real-time navigation solutions.

REFERENCES

[1] Montenbruck O., Markgraf M.; "User's Manual for the Phoenix GPS Receiver"; DLR/GSOC; GTN-MAN-0120; Issue 1.7, 06 June 2006.

[2] Yunck T.P.; "Orbit Determination"; in Parkinson B.W., Spilker J.J. (eds.); *Global Positioning System: Theory and Applications*. AIAA Publications, Washington D.C. (1996).

[3] Berthias J. P., Broca P. ; Comps A., Gratton S., Laurichesse D., Mercier F.; "Lessons learned from the use of a GPS receiver in less than optimal conditions"; 16th International Symposium on Space Flight Dynamics; 3-6 Dec 2001; Pasadena, California (2001)

[4] Goldstein D. B., Born G. H., Axelrad P.; "Real-Time, Autonomous, Precise Orbit Determination Using GPS"; *Navigation - Journal of The Institute of Navigation*; **48/3**, 155-168 (2001).

[5] Montenbruck O., Gill E.; *Satellite Orbits - Models, Methods and Applications*; Springer Verlag, Heidelberg; (2000).

[6] "GRACE Gravity Model GGM01"; Center for Space Research, University of Texas; Austin, 2003. http://www.csr.utexas.edu/grace/gravity/ ggm01/GGM01_Notes.pdf

[7] Brown R.G., Hwang P.Y.C.; *Introduction to Random Signals and Applied Kalman Filtering*; John Wiley & Sons, New York, 3rd ed. (1997).

[8] Tapley B.D., Schutz B.E., Born G.H.; *Statistical Orbit Determination*; Elsevier Academic Press (2004).

[9] Montenbruck O., Gill E.; "State Interpolation for On-board Navigation Systems"; *Aerospace Science and Technology* 5, 209-220 (2001).

[10] Gill E., Montenbruck O., Kayal H.; "The BIRD Satellite Mission as a Milestone Towards GPS-based Autonomous Navigation"; *Navigation - Journal of the Institute of Navigation* **48/2**, 69-75 (2001).

[11] Montenbruck O., Garcia-Fernandez M.; Performance Testing of the MosaicGNSS Receiver for ADM-Aeolus; AEO-DLR-TST-010; Deutsches Zentrum für Luft- und Raumfahrt, Oberpfaffenhofen (2005).

[12] Warren D.L.M., Raquet J.F.; "Broadcast vs. precise GPS ephemerides: a historical perspective"; *GPS Solutions* **7**, 151–156 (2003).

[13] Creel T, Dorsey A. J., Mendicki P.J., Little J., Mach R.G., Renfro B. A.; "The Legacy Accuracy Improvement Initiative"; *GPS World* **17/3**,.20 (2006).

[14] Lear W.M.; *GPS Navigation for Low-Earth Orbiting Vehicles*; NASA 87-FM-2, Rev. 1; JSC-32031, Lyndon B. Johnson Space Center; Houston, Texas (1987).

[15] K.Gantois, O. Montenbruck, F.Teston, P.Vuilleumier, P.v.d.Braembussche, M. Markgraf; "PROBA-2 Mission and New Technologies Overview"; Small Satellite Systems and Services - The 4S Symposium; 25-29 September 2006; Chia Laguna Sardinia, Italy (2006).